Research Article | Vol. 26, No. 8 | 16 Apr 2018 | OPTICS EXPRESS 9565
Optics EXPRESS

Short pulse generation from a passively mode-locked fiber optical parametric oscillator with optical time-stretch

YI QIU,[1,*] XIAOMING WEI,[2] SHUXIN DU,[1] KENNETH K. Y. WONG,[2] KEVIN K. TSIA,[2] AND YIQING XU[2,3]

[1]*School of Engineering, Huzhou University, Huzhou, Zhejiang, China*
[2]*Department of Electrical and Electronic Engineering, The University of Hong Kong, Pokfulam Road, Hong Kong, China*
[3]*College of Information Science and Electronic Engineering, Zhejiang University, Hangzhou, Zhejiang, China*
**yiqiu@connect.hku.hk*

Abstract: We propose a passively mode-locked fiber optical parametric oscillator assisted with optical time-stretch. Thanks to the lately developed optical time-stretch technique, the onset oscillating spectral components can be temporally dispersed across the pump envelope and further compete for the parametric gain with the other parts of onset oscillating sidebands within the pump envelope. By matching the amount of dispersion in optical time-stretch with the pulse width of the quasi-CW pump and oscillating one of the parametric sidebands inside the fiber cavity, we numerically show that the fiber parametric oscillator can be operated in a single pulse regime. By varying the amount of the intracavity dispersion, we further verify that the origin of this single pulse mode-locking regime is due to the optical pulse stretching and compression.

OCIS codes: (190.4970) Parametric oscillators and amplifiers; (140.4050) Mode-locked lasers.

References and links

1. G. P. Agrawal, *Nonlinear Fiber Optics* (Academic).
2. T. Torounidis and P. Andrekson, "Broadband Single-Pumped Fiber-Optic Parametric Amplifiers," IEEE Photonics Technol. Lett. **19**(9), 650–652 (2007).
3. Y. Q. Xu, S. G. Murdoch, R. Leonhardt, and J. D. Harvey, "Raman-assisted continuous-wave tunable all-fiber optical parametric oscillator," J. Opt. Soc. Am. B **26**(7), 1351–1356 (2009).
4. Y. Q. Xu and S. G. Murdoch, "High conversion efficiency fiber optical parametric oscillator," Opt. Lett. **36**(21), 4266–4268 (2011).
5. Y. Q. Xu, K. F. Mak, and S. G. Murdoch, "Multiwatt level output powers from a tunable fiber optical parametric oscillator," Opt. Lett. **36**(11), 1966–1968 (2011).
6. J. M. Chavez Boggio, S. Zlatanovic, F. Gholami, J. M. Aparicio, S. Moro, K. Balch, N. Alic, and S. Radic, "Short wavelength infrared frequency conversion in ultra-compact fiber device," Opt. Express **18**(2), 439–445 (2010).
7. P. Kylemark, P. O. Hedekvist, H. Sunnerud, M. Karlsson, and P. A. Andrekson, "Noise characteristics of fiber optical parametric amplifiers," J. Lightwave Technol. **22**(2), 409–416 (2004).
8. D. R. Solli, G. Herink, B. Jalali, and C. Ropers, "Fluctuations and correlations in modulation instability," Nat. Photonics **6**(7), 463–468 (2012).
9. S. Yang, K. K. Y. Cheung, Y. Zhou, and K. K. Y. Wong, "Tunable single-longitudinal-mode fiber optical parametric oscillator," Opt. Lett. **35**(4), 481–483 (2010).
10. S. Yang, Y. Zhou, J. Li, and K. K. Y. Wong, "Actively Mode-Locked Fiber Optical Parametric Oscillator," IEEE J. Sel. Top. Quantum Electron. **15**(2), 393–398 (2009).
11. J. Zhao, B. Luo, W. Pan, L. Yan, L. Shao, X. Zou, J. Ye, H. Zhu, and Z. Chen, "Characterization of a FM actively mode-locked fiber optical parametric oscillator," J. Opt. Soc. Am. B **33**(7), 1382–1387 (2016).
12. Y. Deng, Q. Lin, F. Lu, G. P. Agrawal, and W. H. Knox, "Broadly tunable femtosecond parametric oscillator using a photonic crystal fiber," Opt. Lett. **30**(10), 1234–1236 (2005).
13. T. Gottschall, J. Limpert, and A. Tünnermann, "Ultra-short pulse fiber optical parametric oscillator," Opt. Lett. **42**(17), 3423–3426 (2017).
14. C. Gu, H. Wei, S. Chen, W. Tong, and J. E. Sharping, "Fiber optical parametric oscillator for sub-50 fs pulse generation: optimization of fiber length," Opt. Lett. **35**(20), 3516–3518 (2010).

#320019 https://doi.org/10.1364/OE.26.009565
Journal © 2018 Received 18 Jan 2018; revised 21 Mar 2018; accepted 22 Mar 2018; published 3 Apr 2018

Optics EXPRESS

15. E. S. Lamb, S. Lefrancois, M. Ji, W. J. Wadsworth, X. S. Xie, and F. W. Wise, "Fiber optical parametric oscillator for coherent anti-Stokes Raman scattering microscopy," Opt. Lett. **38**(20), 4154–4157 (2013).
16. G. Cappellini and S. Trillo, "Third-Order Three-Wave Mixing in Single-Mode Fibers - Exact-Solutions and Spatial Instability Effects," J. Opt. Soc. Am. B **8**(4), 824–838 (1991).
17. U. Keller, K. J. Weingarten, F. X. Kartner, D. Kopf, B. Braun, I. D. Jung, R. Fluck, C. Honninger, N. Matuschek, and J. A. Au, "Semiconductor saturable absorber mirrors (SESAM's) for femtosecond to nanosecond pulse generation in solid-state lasers," IEEE J. Sel. Top. Quantum Electron. **2**(3), 435–453 (1996).
18. B. Ortaç, M. Plötner, J. Limpert, and A. Tünnermann, "Self-starting passively mode-locked chirped-pulse fiber laser," Opt. Express **15**(25), 16794–16799 (2007).
19. S. Rui, C. Hong-Wei, C. Sheng-Ping, H. Jing, and L. Qi-Sheng, "A SESAM passively mode-locked fiber laser with a long cavity including a band pass filter," J. Opt. **13**(3), 035201 (2011).
20. M. Pessot, P. Maine, and G. Mourou, "1000 times expansion/compression of optical pulses for chirped pulse amplification," Opt. Commun. **62**(6), 419–421 (1987).
21. J.-L. Wu, Y.-Q. Xu, J.-J. Xu, X.-M. Wei, A. C. S. Chan, A. H. L. Tang, A. K. S. Lau, B. M. F. Chung, H. Cheung Shum, E. Y. Lam, K. K. Y. Wong, and K. K. Tsia, "Ultrafast laser-scanning time-stretch imaging at visible wavelengths," Light Sci. Appl. **6**(1), e16196 (2017).
22. Y. R. Shen, *The Principles of Nonlinear Optics* (J. Wiley).
23. J. F. Philipps, T. Töpfer, H. Ebendorff-Heidepriem, D. Ehrt, and R. Sauerbrey, "Spectroscopic and lasing properties of Er3+:Yb3+-doped fluoride phosphate glasses," Appl. Phys. B **72**(4), 399–405 (2001).
24. B. H. Kolner, "Space-time duality and the theory of temporal imaging," IEEE J. Quantum Electron. **30**(8), 1951–1963 (1994).
25. H. A. Haus, J. G. Fujimoto, and E. P. Ippen, "Analytic theory of additive pulse and Kerr lens mode locking," IEEE J. Quantum Electron. **28**(10), 2086–2096 (1992).
26. K. Goda, D. R. Solli, K. K. Tsia, and B. Jalali, "Theory of amplified dispersive Fourier transformation," Phys. Rev. A **80**(4), 043821 (2009).
27. M. A. Soto, M. Alem, M. Amin Shoaie, A. Vedadi, C.-S. Brès, L. Thévenaz, and T. Schneider, "Optical sinc-shaped Nyquist pulses of exceptional quality," Nat. Commun. **4**, 2898 (2013).

1. Introduction

Parametric amplification in optical fibers is a nonlinear process which converts a strong pump laser into a small signal [1]. During the parametric amplification process, the wavelengths of the pump and signal must fulfill the phase-matched condition which is determined by the balance between dispersion and nonlinearity in the parametric gain fiber to maximize the energy conversion, and it is different from the other conventional fiber optical amplifiers, such as Erbium-doped fiber amplifier and Raman amplifier [2]. Essentially, this implies that the parametric gain can be tailored to any wavelength region by choosing a fiber with an appropriated dispersion as well as a proper pump wavelength. Thus, wide tunability can be easily achieved by tuning the wavelength of the pump laser near the zero-dispersion-wavelength of the parametric gain fiber. This wide tunable gain has been well demonstrated in fiber optical parametric oscillators (FOPOs), and a gain bandwidth of over 240 nm can be obtained by using a continuous-wave (CW) pumping scheme [3]. Thanks to the adjustable parametric gain of the parametric process and the development of the highly nonlinear fibers, many FOPOs have been demonstrated over various wavelength regions to provide extremely high output power with high conversion efficiency [4–6]. Notably, the oscillation of the signal inside the cavity is initiated from quantum noise, and the incoherence of the noise will be inherited by the oscillating signal [7, 8]. As a result, people have endeavored for developing highly coherent output from FOPOs, such as generating a single longitudinal mode inside a FOPO [9]. On the other hand, mode-locking the oscillating signal has also been demonstrated to generate short pulses in FOPOs using the active mode-locking technique in which the oscillating signal is synchronously modulated to match the cavity length of the FOPOs [10, 11]. Although the ultrashort pulses generated from FOPOs have been demonstrated using an ultrashort pulse as the pump, this type of ultrashort pulse generation can only be considered as inheriting the small temporal envelope of the pump in which the parametric gain is confined [12–15]. Essentially, there is no mode-locking mechanism which enforces the phases between the oscillating longitudinal modes in this type of ultrashort pulsed pump FOPOs. Moreover, the tunability of the FOPO is inevitably limited by the temporal walk-off between the ultrashort pump pulse and oscillating sideband. To this end, a

Optics EXPRESS

CW or quasi-CW pump needs to be considered when implementing a true passively mode-locked FOPO. Especially, using a CW or quasi-CW pump can further reduce the complexity when designing the pumping scheme of a FOPO.

In this work, we initially address the difficulty of implementing a passively mode-locked FOPO by comparing it with the conventional fiber mode-locked laser using the space-time analogy. After introducing the time-stretch into the optical cavity, which in practice is to manage the dispersion arrangement of the cavity, we numerically show that using a conventional saturable absorber acting as a temporal Kerr lens pinhole, and it is feasible to generate an ultrashort pulse via the passive mode-locking in a FOPO. By adjusting the amount of dispersion in the oscillating cavity, we show that the passively mode-locked FOPO can be operated in either a single pulse or multiple pulses regime. Finally, we interpret the output temporal and spectral profiles of this the passively mode-locked FOPO as a result of a direct mapping of the pump temporal intensity profile.

2. Theory

We consider implementing the passive mode-locking in a singly resonant FOPO in which one of the parametric sidebands is circulating inside the FOPO feedback loop cavity, as shown in Fig. 1. For the sake of simplicity, we only consider the scalar parametric process and assume that all optical fields inside the FOPO are co-linearly polarized, and we neglect the vector parametric process as well. We also omit the Raman effect inside the parametric gain fiber and only consider the pure Kerr effect as the origin of the parametric gain by considering the frequency detuning of the sidebands being relatively far away from the Raman gain peak. The following part of this section will describe in details how the operating conditions of each component of the FOPO to achieve the passive mode-locking.

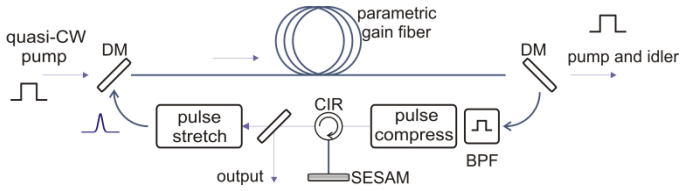

Fig. 1. A generic setup of a passively mode-lock fiber parametric laser. DM: dichroic mirror, BPF: band pass filter, CIR: circulator, SESAM: semiconductor saturable absorber mirror.

2.1 Quasi-CW pump and parametric gain fiber

The quasi-CW pump is generated by intensity-modulating a monochromatic CW pump into a square pulse with a pulse width in the order of the nanosecond. Within the range of this pulse width, it is sufficient to claim that the pump used in the parametric process is a quasi-CW pump. In practice, this can be simply achieved with an intensity modulator, and the peak power of the modulated pulse can be boosted up by amplifying with a rare earth doped fiber amplifier. The pump only propagates inside the parametric gain fiber and exits the cavity at the end of the parametric gain fiber. The selection of the pump wavelength is realized by using a pair of dichroic mirrors (DMs), which also minimize the overall cavity loss of the oscillating sideband. And the noise with the phase-matched frequency will experience parametric gain and grow exponentially within the pump envelope. However, since the parametric process is an energy conversion process, the maximum power that can be obtained by the two sidebands is limited by the total power of the pump and the phase mismatch. At the phase-matched frequency, the maximum conversion efficiency from the pump to each sideband is 20% [16].

2.2 Intracavity filtering

For a singly resonant FOPO, a wide-band tunable intracavity filter is commonly used to select the central wavelength and the bandwidth of the oscillating sideband. The intracavity filtering

Optics EXPRESS

has several purposes: (i) Since the parametric process is a frequency-sensitive process, the power conversion efficiency from the pump to the sidebands will strongly depend on the phase mismatch between the pump and the sidebands. This can be adjusted by selecting the gain region within the parametric gain sidelobes. (ii) The pulse width of the oscillating sideband after the optical time-stretch process depends on the amount of dispersion in the oscillating cavity as well as the spectral width which needs to satisfy the condition related to the amount of dispersion in order to operate the FOPO in a single pulse regime. We will discuss in details the relationship between the mode-locked spectral width and the amount of dispersion in the time-stretch process in the later subsections.

2.3 Saturable absorber

The passive mode-locking process in this parametric oscillator is realized by using a semiconductor saturable absorber mirror (SESAM) which is commonly used in the other rare earth doped fiber mode-locked lasers and Q-switch lasers [17–19]. The rate of reflection of the SESAM can be simply modeled as

$$r = 1 - \frac{\alpha}{1 + P / P_{sat}}, \tag{1}$$

where α is the linear absorption of the SESAM, P is the instantaneous power of the optical field, and P_{sat} is the saturable power of the SESAM. Although artificial saturable absorbers, e.g., nonlinear polarization rotation and fiber loop mirror can result in the similar effect in shaping the oscillating sideband in the cavity, the cavity length or the dispersion profile of the cavity won't be modified by the SESAM. Primarily, the key point of the mode-locking in this work lies on the pulse stretching and compression inside the cavity. Thus, unless specified we only consider using the SESAM as the mode-locking element in this paper.

2.4 Pulse stretching and compressing

Note that the parametric process is an energy conversion process, so that the maximum power of the sideband cannot exceed the power of the pump. Once the conversion efficiency reaches the maximum, the sidebands start to transfer the power back to the pump. This is in contrast to the gain process in the rare earth doped fibers which has a long upper-state lifetime, and it allows the intracavity field to accumulate sufficient energy before returning to the ground state. Thus, to efficiently harvest the energy from the pump without further recurrence, we adopt the chirped-pulse-amplification technique which has been commonly used in short pulse amplification to our passively mode-locked FOPO [20]. As shown in Fig. 1, the scheme we proposed is to time-stretch the oscillating pulse before the parametric gain fiber. The pulse needs to be greatly stretched to match the pulse envelope of the modulated pump as

$$D_{\text{total}} \cdot \Delta\Omega \approx \tau_{\text{pump}}, \tag{2}$$

where $\Delta\Omega$ is the spectral width of the oscillating sideband which is set by the intracavity filtering, τ_{pump} is the pulse width of the intensity modulated pump, and D_{total} is the dispersion coefficient of the dispersive element. The dispersive component that we use to accomplish the time-stretch process is named as free-space angularly chirp-enhanced delay cavity (FACED) [21]. There are two reasons why this device is chosen for the time-stretch process: (i) the amount of dispersion induced by a FACED is configurable such that the pulse width of oscillating sideband after the time-stretch process can be matched with the pulse width of the pump as described in Eq. (2) above. Later we will discuss the effect of the amount of dispersion on the stability of the mode-locking process. (ii) The optical path length to induce such a large amount of dispersion using a FACED is extremely small comparing to the length of using other time-stretching technique, e.g., fiber dispersion. Thus, using a FACED as the dispersive element effectively reduces the overall length of the cavity as well as the

Optics EXPRESS

detrimental nonlinear effects, and it allows the mode-locked pulse to operate in a more stable regime. After going through the parametric gain fiber, the oscillating sideband will be compressed by another FACED with the same amount of dispersion but with opposite sign before the SESAM. Thus, those oscillating spectral components with proper phases, i.e., maximizing the peak power after the compression, will be automatically selected by the SESAM and become dominated in the following oscillations.

2.5 Space-time analogy

To further illustrate the underlining mechanisms between the fiber mode-locked rare-earth-doped fibers and the passively mode-locked FOPO, we depict their corresponding space-time diagrams in Fig. 2. The oscillating process of the intracavity pulse can be simplified as a periodic propagation over a same round trip cavity, and the axis is the propagation time/distance. We first note that the parametric process in optical fibers is an instantaneous process, which implies that the onset oscillating sideband will experience extremely short "upper-state" lifetime time in the parametric gain fibers when comparing with that in the rare earth doped gain fibers [22, 23]. Thus the noises in the parametric gain fiber are essentially stationary with respect to the group velocity frame of the pump envelope of FOPOs, and they experience equal amounts of parametric gain. The oscillation will reach the equilibrium once the oscillating noises reach the saturation power which is set by the pump power and the phase-matched condition [16]. In order to generate a short pulse in a FOPO, it is necessary to require the pump to be a high peak power ultrashort pulse as used in those pulsed pump FOPOs which were mentioned in the introduction. In contrast, in the rare earth doped fiber the onset noise with the correct phases will dominate and harvest the entire gain as the long lifetime allows the "propagating" pulse to be continuously amplified without competing with other noise as shown in Fig. 2(a).

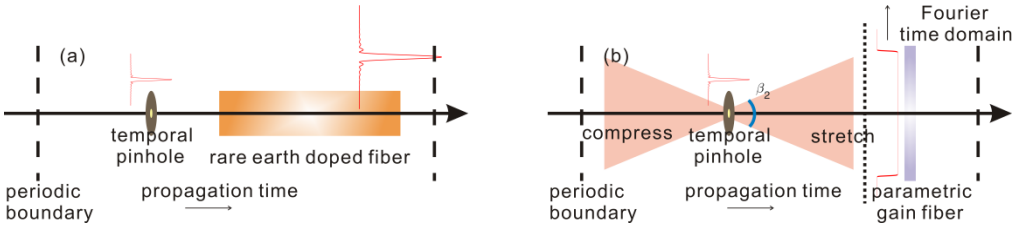

Fig. 2. Space-time analogy of passively mode-locked lasers with a rare earth doped gain fiber (a) and a parametric gain fiber (b).

To overcome the gain constraint in the parametric process in optical fibers, we here introduce the optical time-stretch technique into the optical cavity before and after the mode-locked element, i.e., temporal pinhole, as shown in Fig. 2(b). In the space-time duality, the optical time-stretch process of an optical pulse is analog to the paraxial diffraction from a spatial pinhole [24]. Providing that the propagation distance is sufficiently large, the far-field diffraction pattern will become the Fourier transform of the optical field after the pinhole. Meanwhile, the mode-locked element used in the passive mode-locking are analog to the Kerr lensing used in the free-space mode-locked lasers in which the transmission of the oscillating pulse becomes nonlinear when the pulse energy is sufficiently high [25]. The spectral gain is analog to the aperture size of the gain medium at the far-field diffraction. Here we would like to point out that the same amount of dispersion with opposite sign induced by the FACED is equivalent to propagate the phase conjugated far-field. In this case, the pinhole is again to select the spectral components with the appropriate phases while the diffracting and reversed diffracting processes are respectively, to spread out the spectral components across the entire parametric gain medium, and to reverse the spreading for a high intensity before Kerr lensing. Thus, the spreading of the spectral components effectively lowers the saturation power of the

Optics EXPRESS

pump and further allows the "stationary" noise to spread and compete with other parts of the noise under the pump envelope.

3. Numerical simulations

To demonstrate the performance of our proposed fiber parametric mode-locked laser, we numerically simulate the evolution of the optical pulse using the nonlinear Schrodinger equation. The integration of the optical field is computed using the split-step method [1]. We consider a quasi-CW pump with a square pulse width of 1 ns and a peak power of 6 W. The parametric gain fiber is a 50 m-long highly nonlinear fiber with a nonlinear coefficient of γ = 10 W^{-1}/km, and the dispersion coefficients at the central frequency are β_2 = –0.1 ps^2/km, β_3 = 0.15 ps^3/km, β_4 = -7.1×10^{-4} ps^3/km. The frequency detuning of corresponding phase-matched sidebands is 4.4 THz at the peak pump power of 6 W. The linear absorption coefficient and the saturable power of the SESAM are set to α = 0.9 and P_{sat} = 1000 W, respectively. Excluding the loss from the SESAM, the rest of the intracavity loss for the oscillating sideband is set to 50%. The intracavity filter is centered at the phase-matched frequency with an FWHM of 0.5 THz. As described by Eq. (2), the stretched pulse width of the oscillating sideband before the parametric gain fiber is determined by its spectral width and the amount of the dispersion induced by the FACED. The amount of dispersion induced by the FACED before the parametric gain fiber is initially set to 318 ps^2. Owning to the large dispersion from FACEDs, the amount of dispersion is equivalent to the dispersion from a length of 16 km of single mode fiber (SMF) with a second-order dispersion coefficient of 20 ps^2/km. The FACED after the parametric gain fiber is set to the same amount of dispersion but with an opposite sign to recompress the stretched pulse.

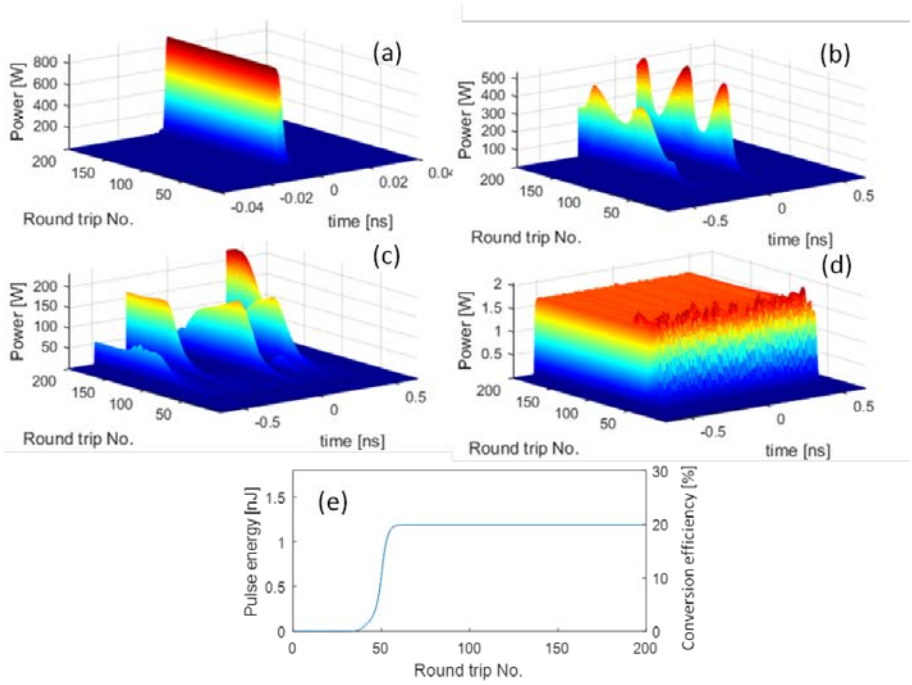

Fig. 3. Temporal evolution of intracavity pulses, with various amount of dispersion induced by the FACED cavity (a) 318 ps^2, (b) 127 ps^2, (c) 64 ps^2, and (d) no dispersion arrangement. (e) is the pulse energy and the conversion efficiency from the pump to mode-locked sideband as a function of round trip number in the single pulse regime.

Optics EXPRESS

3.1 Result

We plot the temporal evolutions of the oscillating sideband as a function of the round trip number in Figs. 3(a)-3(d) with various amounts of dispersion as well as no dispersion introduced in the oscillating cavity, respectively. As shown in Fig. 3(a), a single pulse is generated from the noise level, and its power grows up significantly around 50 round trips, with a saturated peak power of 890 W. When comparing with the other cases shown in Figs. 3(b) and 3(c) in which the insufficient amounts of dispersion are provided before and after the parametric gain fiber, mode-locked pulses become unstable with much lower peak power and go into a multiple pulses regime. Note that the amount of dispersion in Figs. 3(b) and 3(c) are chosen to be 40% and 20% respectively of the amount of dispersion to perform a fully stretched and compressed as of in Fig. 3(a). As a result, the number of subpulses in the unstable multiple pulses regimes is approximately equal to the reciprocal of these fraction numbers. This can be explained by the fact that for a perfect single pulse, all spectral components before entering the parametric gain fiber need to be distributed across the entire envelope of the pump via the pulse stretching, and the power of each spectral component can reach equilibrium when oscillating inside the cavity. However, when the dispersion is insufficient such that the spectral components cannot be distributed across the entire pump envelope, the noise that is phase-matched with the pump but beyond the initially oscillating spectral components can also start building up the power and oscillating, and they become the subpulses under the pump envelope. For the case without any dispersion arrangement shown in Fig. 3(d), the sideband only duplicates the envelope of the pump pulse with the maximum conversion efficiency of 20% at the phase-matched frequency. Figure 3(e) shows the pulse energy and the conversion efficiency from the pump to the oscillating sideband of the single pulse regime. Note that while the pulse energy in the multiple pulses regime is too complicated to estimate, the total conversion efficiency in the multiple pulses regime is identical to that in the single pulse regime. The amount of the intracavity dispersion effectively modifies the energy distribution of the optical field while it does not affect the conversion efficiency of the oscillator.

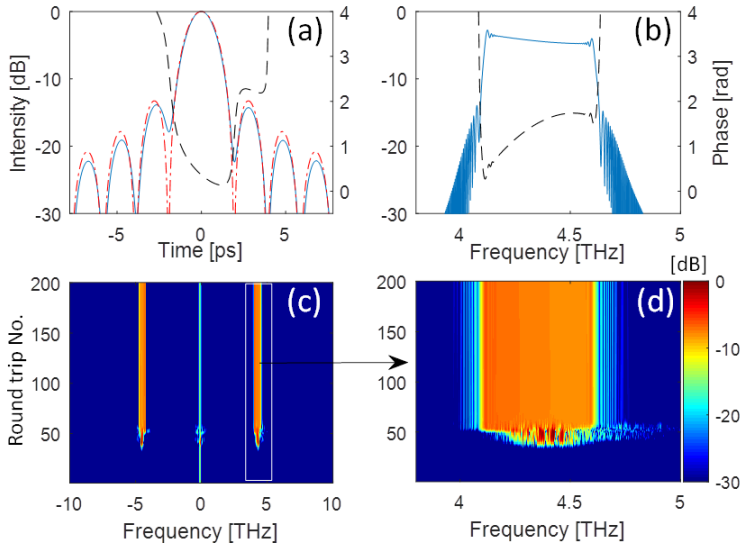

Fig. 4. (a) and (b) are, respectively the temporal and spectral intensity/phase of the intracavity pulse. The solid curves are the simulated temporal and spectral intensity, and the dashed-dot curve in (a) is the theoretical sinc function profile. Dashed curves are the corresponding temporal and spectral phase. (c) is the overall spectral evolution of the oscillator. (d) is the close-up view of the spectral evolution of the intracavity mode-locked sideband indicated by the squared box in (c).

Optics EXPRESS

We now further analyze the pulse profile from the single pulse regime. We plot in Figs. 4(a) and 4(b) respectively, the temporal and spectral intensity profiles in log scale and the corresponding phase when the single pulse regime reaches the stable state. The temporal intensity plotted as the solid curve in Fig. 4(a) resembles closely a sinc function profile comparing with the theoretical fitting of the dashed-dot curve, with an almost flat chirp (dashed curve) across the main pulse; while the spectral profile in Fig. 4(b) is nearly a flat top rectangular shape which is corresponding to Fourier transform of the sinc function. The FWHM of the temporal pulse width is 1.6 ps, and the spectral width is set by the intracavity filter which is 0.5 THz. The time-bandwidth product (TBP) of the sinc function pulse is 0.8, while the theoretical TBP of the sinc function pulse can be readily determined and is equal to 0.89, indicating that the single pulse after mode-locking the FOPO is a nearly transform-limited pulse. The physical mechanism of generating such a sinc pulse can be interpreted as that the spectral components are mapped into the temporal domain through the time-stretch process and evenly distributed within the pump envelope. The time-stretch process here is effectively the dispersive Fourier transform process, and the spectrum of the mode-locking pulse is being amplified and duplicating the temporal profile of the pump whose power is being converted into the power of these spectral components [26]. We would like to point out that the scheme of generating the sinc function pulse proposed in this work can significantly reduce the complexity of the recently developed Nyquist-sinc pulse generation [27]. We further observe the intracavity spectral evolution of the single pulse mode-locking as shown in Figs. 4(c) and 4(d). Figure 4(c) shows the sidebands generation process at the output the FOPO and the power of the sidebands have grown significantly about 50 round trips, and Fig. 4(d) shows the close-up view of the oscillating sideband. After 50 round trips when the pulse accumulated sufficient energy, the unstable sideband suddenly becomes broadened which indicates the onset of the mode-locked process and the spectrum eventually becomes a flat top spectrum.

4. Summary

In summary, we have presented a numerical study of a passively mode-locked fiber optical parametric oscillator pumped with a quasi-CW pump. We have shown that the amount of dispersion is critical for efficiently harvesting the parametric gain from the quasi-CW pump. The operation of the single pulse regime has been demonstrated through the numerical simulation with the stretched pulse width of the oscillating sideband matched with the pulse width of the pump. By mismatching the amount of dispersion in the time-stretch/compression, we have shown that the oscillation can fall into a multiple pulses regime. In the single pulse regime, the short pulse exhibits a perfect sinc pulse profile which is the result of duplicating the pump pulse intensity profile at which the spectral components were being amplified during the time-stretching and compressing processes.

Funding

School of Engineering, Huzhou University; the Basic Public Welfare Research Project in Zhejiang Province (LGG18F030009).